

# The Synergistic Anti-tumor Effect of Iodine-125 Low-dose-rate Brachytherapy and Anti-PD-1 Therapy on Lung Cancer in Mice

**Yiyi Cao**

The First Affiliated Hospital of Chongqing Medical University

**Wenbo Li**

The First Affiliated Hospital of Chongqing Medical University

**Jia Li**

the First Affiliated Hospital of Chongqing Medical University

**Yu Weng**

The First Affiliated Hospital of Chongqing Medical University

**Chang Chen**

The First Affiliated Hospital of Chongqing Medical University

**ZhengJie Wang**

The First Affiliated Hospital of Chongqing Medical University

**Hua Pang** (✉ [phua1973@163.com](mailto:phua1973@163.com))

Department of Nuclear Medicine, the First Affiliated Hospital of Chongqing Medical University, Chongqing, 400016, China <https://orcid.org/0000-0001-6601-3208>

---

## Research

**Keywords:** Radiotherapy, Brachytherapy, PD-1/PD-L1, Immunotherapy

**Posted Date:** November 6th, 2020

**DOI:** <https://doi.org/10.21203/rs.3.rs-102600/v1>

**License:** © ⓘ This work is licensed under a Creative Commons Attribution 4.0 International License.

[Read Full License](#)

---

# Abstract

**Background:** Radiotherapy (RT) when combined with anti-PD-1 therapy has a significant effect, but RT fractionation and dose impact the effects of this combined therapy. Iodine-125 particle implantation ( $^{125}\text{I}$  RPI) is a hyperfractionated low-dose-rate brachytherapy. Its impact on the tumor immune microenvironment and the efficacy of  $^{125}\text{I}$  RPI combined with anti-PD-1 therapy are unknown. In this study, we evaluated the effectiveness of  $^{125}\text{I}$  RPI combined with anti-PD-1 therapy and their impact on tumor immunity.

**Methods:** A Lewis lung cancer (LLC) mouse model was established and radioactive iodine-125 particles were implanted into the tumors. Tumor tissues were obtained six and 12 days after particle implantation, and the expression of PD-1/PD-L1 was detected by flow cytometry. On day 0, LLC cells were injected subcutaneously into the right hindlimb (primary tumor) and left flank (secondary tumor) of mice. On day 10, the mice were randomly divided into PBS,  $\alpha$ -PD-1,  $^{125}\text{I}$  RPI, and  $\alpha$ -PD-1+ $^{125}\text{I}$  RPI groups. On day 22, tumor tissues were extracted from the mice. The proportion of immune cell subsets in the tumor immune microenvironment was detected by flow cytometry, and the primary and secondary tumor volumes were monitored.

**Results:** After  $^{125}\text{I}$  RPI, the expression of PD-L1 on tumor cells was upregulated ( $P < 0.0001$ ), and the proportion of CD8+ PD-1+ T cells also increased ( $P = 0.0001$ ).  $^{125}\text{I}$  RPI combined with anti-PD-1 therapy synergistically inhibited primary ( $P = 0.0139$ ) and secondary ( $P = 0.0494$ ) tumor growth. The flow cytometry results showed that the combination therapy could increase the proportion of CD8+ T cells ( $P = 0.0055$ ) and decrease the proportion of T regulatory cells ( $P < 0.0227$ ) in the tumor microenvironment. Survival analysis shows that the sequence of  $^{125}\text{I}$  RPI and  $\alpha$ -PD-1 affects efficacy, and early initiation of  $^{125}\text{I}$  RPI is more beneficial.

**Conclusion:**  $^{125}\text{I}$  RPI combined with anti-PD-1 therapy can significantly inhibit tumor growth and activate anti-tumor immunity, which present a promising approach for the treatment of cancer.

## Introduction

Radiotherapy (RT) when combined with anti-PD-1 therapy has a significant effect, but RT fractionation and dose impact the effects of this combined therapy. Iodine-125 particle implantation ( $^{125}\text{I}$  RPI) is a hyperfractionated low-dose-rate brachytherapy. Its impact on the tumor immune microenvironment and the efficacy of  $^{125}\text{I}$  RPI combined with anti-PD-1 therapy are unknown. In this study, we used a mouse model of LLC to evaluate the effect of  $^{125}\text{I}$  RPI on the PD-1/PD-L1 axis, the efficacy of  $^{125}\text{I}$  RPI combined with anti-PD-1 therapy, and the effect of combined therapy on the proliferation and function of T-lymphocytes. We also investigated the effect of the treatment sequence on their efficacy to provide preclinical evidence for hyperfractionated brachytherapy combined with anti-PD-1/PD-L1 therapy.

The synergistic anti-tumor effect of iodine-125 low-dose-rate brachytherapy and anti-PD-1 therapy on lung cancer in mice

PD-1/PD-L1 is a major immunosuppressive molecule in the (1). PD-L1 expressed on tumor cells can bind PD-1 on activated T cells and leads to T cell exhaustion, thus preventing immune killing of tumor cells(2). Anti-PD-1/PD-L1 treatment can eliminate immunosuppression and activate anti-tumor immunity. Clinical studies have shown that anti-PD-1/PD-L1 therapy has been applied to a variety of advanced tumors with significant efficacy(3).

Radiotherapy (RT) is an indispensable method used in the treatment of cancer. In recent years, increasing attention has been paid to the impact of RT on tumor immunity. Studies have found that RT can also reduce the size of tumors outside of the radiation field; this is known as the abscopal effect(4). The abscopal effect occurs when RT enhances the anti-tumor immune response. RT can promote the expression of tumor-associated antigens and neoantigens(5–7), making the irradiated tumor an “in situ vaccine”(8). RT can also induce damage-associated molecular patterns, including changes in molecules such as ATP, calreticulin, and the high mobility group of B1 proteins that can promote antigen uptake and presentation(9–11). However, the abscopal effect is rare in clinical practice. This is because RT can upregulate the expression of immunosuppressive molecules such as PD-L1 and T regulatory cells (Tregs) (12, 13). This negative regulatory effect on immunity means that the immune activation effect of RT is not sufficient to disrupt the immunosuppressive state of the tumor microenvironment. Studies have shown that RT and anti-PD-1/PD-L1 therapy have a synergistic effect, and combination therapy can reverse the immunosuppressive state(14, 15).

RT fractionation (conventional fractionated, hypofractionated, and single-dose) and dose have different effects on tumor immunity, and are key factors affecting the efficacy of RT when combined with immunotherapy(16, 17). Dewan et al. showed that fractionated RT could induce the abscopal effect when combined with anti-CTLA-4 treatment, whereas single-dose RT did not induce the abscopal effect(16). <sup>125</sup>I particle implantation (<sup>125</sup>I RPI) is a type of hyperfractionated low-dose-rate brachytherapy, which is widely used to treat various solid tumors, including cancer of the lung, pancreas, liver, prostate, bladder, and rectum(18–21). Currently, the impact of <sup>125</sup>I RPI on the tumor immune microenvironment is poorly understood, and no studies exist on hyperfractionated RT combined with immunotherapy. In addition, most studies used external beam RT (EBRT) combined with immunotherapy(22–24), and studies of brachytherapy combined with immunotherapy are rare. In this study, we investigated its efficacy.

In this study, we used a mouse model of LLC to evaluate the effect of <sup>125</sup>I RPI on the PD-1/PD-L1 axis, the efficacy of <sup>125</sup>I RPI combined with anti-PD-1 therapy, and the effect of combined therapy on the proliferation and function of T-lymphocytes. We also investigated the effect of the treatment sequence on their efficacy to provide preclinical evidence for hyperfractionated brachytherapy combined with anti-PD-1/PD-L1 therapy.

## Materials And Methods

## Cell lines

LLC cells were purchased from the Cell Bank at Shanghai Institute of Cell Biology, Chinese Academy of Science. LLC cells were cultured in DMEM high glucose medium with 10% fetal bovine serum (both from GIBCO, Thermo Fisher Scientific, Waltham, MA, USA) and incubated in a 5% CO<sub>2</sub> incubator at 37 °C. All cells were cultured for a limited passage before implantation.

## Mice and tumor challenge

C57BL/6 female mice, aged 6–8 weeks, were purchased from Experimental Animal Center of Chongqing Medical University. Cells in logarithmic growth phase were collected, and a  $1 \times 10^6$  cell suspension was injected subcutaneously (SC) into the right hindlimb (primary tumor) of mice on day 0, and the left flank (secondary tumor) on day 3. On day 10, when the tumor volume was  $\sim 200 \text{ mm}^3$ , mice were randomly assigned to the phosphate-buffered saline (PBS) group, the <sup>125</sup>I RPI group, the  $\alpha$ -PD-1 group, or the <sup>125</sup>I RPI +  $\alpha$ -PD-1 group. Tumor volume was measured and recorded with vernier calipers every 2–3 days; a tumor volume of  $(\text{length} \times \text{width}^2)/2$  and tumor diameter exceeding 20 mm was taken as the endpoint of the survival analysis.

## Tumor therapy

<sup>125</sup>I RPI therapy: The mice were anesthetized by intraperitoneal (IP) injection of 1% pentobarbital at a dose of 50 mg/kg. After securing the mice, an 18 g needle was inserted into the center of the tumor 0.5 cm away from the tumor edge, and the depth of the needle was measured and marked. The needle core was withdrawn, and a radioactive <sup>125</sup>I particle (0.8 mci, 29.6 MBq) was implanted into the center of the tumor. A cotton ball was used to stop the bleeding once the needle was withdrawn. The mice were reared in single cages, one mouse per cage. The mice were observed, and their food intake, level of activity, and general condition were monitored, and the skin area around the tumor was assessed for signs of redness, swelling, and ulceration.

Anti-PD-1 treatment:  $\alpha$ -PD-1 monoclonal antibody (mAb) (clone RMP1-14; Bio X Cell, Lebanon, NH, USA) was administered by IP injection at a dose of 200  $\mu\text{g}/\text{mouse}$ , once every other day for a total of five times.

## Flow cytometry

The mice were sacrificed and the tumor tissues were cut into sections of  $< 3 \text{ mm}$  in length with ophthalmic scissors. We added 2 ml DMEM high glucose medium containing 1 mg/ml collagenase IV (Sigma-Aldrich, St. Louis, MO, USA), 1 mg/ml hyaluronidase (Solarbio, Beijing, China), and 200 u DNase I (Solarbio) to the sections. The sections were then digested in a shaking device at 37 °C for 1–2 h, and filtered with a 100  $\mu\text{m}$  strainer to obtain a single-cell suspension. After blocking of non-specific binding with  $\alpha$ -CD16/32 Ab, the cells were stained with antibodies against mouse PD-L1, PD-1, CD45, CD8, CD4, and CD25 (BD Pharmingen; BD Biosciences, San Jose, CA, USA) for 30 min in the dark. We used the

Transcription-Factor Buffer Set (BD Pharmingen) for intracellular staining according to the manufacturer's protocol. To stimulate the cells and perform surface and intracellular staining to detect interferon (IFN)- $\gamma$  and tumor necrosis factor (TNF)- $\alpha$ , PMA/ionomycin (MultiSciences Biotech Co. Ltd., Hangzhou City, China) and brefeldin A/monensin (MultiSciences Biotech Co. Ltd.) were added 6 h in advance *in vitro*. Samples were collected on a FACSCalibur Flow Cytometer (BD Biosciences) and data were analyzed using FlowJo software (BD Biosciences).

## Statistical analyses

All statistical analyses were performed using GraphPad Prism software 8.0 (GraphPad Software, Inc., San Diego, CA, USA). Experiments were repeated three times. Measurement data are expressed as means  $\pm$  SEM. Repeated measures analysis of variance was used to compare tumor growth curves. The survival curve was created using the Kaplan–Meier method and analyzed using the log-rank test. Student's t-tests were used for comparisons of the means of two samples. Comparisons of the means of multiple groups were made by one-way ANOVA. A P-value of  $P < 0.05$  was considered to be statistically significant.

# Results

## **$^{125}\text{I}$ RPI upregulated the expression of PD-1/PD-L1 in the TME**

To investigate PD-1/PD-L1 axis involvement in immunosuppression following  $^{125}\text{I}$  RPI treatment, tumor tissues were collected on days 6 and 12 after  $^{125}\text{I}$  RPI treatment. The expression of PD-L1 on tumor cells and PD-1 on CD8 + tumor infiltrating lymphocytes (TILs) was analyzed by flow cytometry. Compared with the control group, the expression of PD-L1 was upregulated in the  $^{125}\text{I}$  RPI group on day 6 ( $P = 0.0053$ ), and further upregulated on day 12 (Fig. 1A and 1B; when compared with expression at day 6 and the control;  $P = 0.0057$  and  $P < 0.0001$ , respectively). On day 6 after  $^{125}\text{I}$  RPI, the expression of PD-1 on CD8 + TILs was not significantly different from that in the control group ( $P = 0.1351$ ), but was upregulated on day 12 (Fig. 1C and 1D;  $P = 0.0001$ ). This shows that following  $^{125}\text{I}$  RPI implantation, as time increased, the number of exhausted T cells increased, and the immune response may have been inhibited by PD-1/PD-L1. Therefore, we speculate that PD-1/PD-L1 blockade therapy may improve the efficacy of  $^{125}\text{I}$  RPI.

## **Combination $^{125}\text{I}$ RPI and anti-PD-1 therapy inhibits tumor growth and induces the abscopal effect**

To test whether combination  $^{125}\text{I}$  RPI and anti-PD-1 therapy inhibited tumor growth and induced the abscopal effect, the mice were divided into the following groups 10 days after tumor inoculation: PBS group,  $^{125}\text{I}$  RPI group,  $\alpha$ -PD-1 group, and  $^{125}\text{I}$  RPI +  $\alpha$ -PD-1 group. On day 10,  $^{125}\text{I}$  particles were implanted, and anti-PD-1 antibodies were injected on days 10, 12, 14, 16, and 18. Anti-PD-1 therapy alone had little effect on tumor volume,  $^{125}\text{I}$  RPI delayed tumor growth, and combined therapy significantly delayed tumor growth ( $P = 0.007$ ,  $\alpha$ -PD-1 vs.  $^{125}\text{I}$  RPI +  $\alpha$ -PD-1 =  $2734.70 \pm 548.16 \text{ mm}^3$  vs.  $1186.16 \pm 218.14 \text{ mm}^3$  on day 22;  $P = 0.0139$ ,  $^{125}\text{I}$  RPI vs.  $^{125}\text{I}$  RPI +  $\alpha$ -PD-1 =  $1921.32 \pm 307.35 \text{ mm}^3$  vs.  $1186.16 \pm 218.14 \text{ mm}^3$  on day 22; Fig. 2A and 2B). In addition, combination therapy inhibited the growth of secondary tumors,

whereas monotherapy did not ( $P = 0.0410$ , anti-PD-1 vs.  $^{125}\text{I}$  RPI +  $\alpha$ -PD-1 =  $2503.2764 \pm 473.71 \text{ mm}^3$  vs.  $1624.67 \pm 155.10 \text{ mm}^3$  on day 22;  $P = 0.0494$ ,  $^{125}\text{I}$  RPI vs.  $^{125}\text{I}$  RPI +  $\alpha$ -PD-1 =  $2621.33 \pm 563.22 \text{ mm}^3$  vs.  $1624.67 \pm 155.10 \text{ mm}^3$  on day 22; Fig. 2C). As shown in Fig. 2D, the median survival time of the PBS,  $^{125}\text{I}$  RPI,  $\alpha$ -PD-1, and  $^{125}\text{I}$  RPI +  $\alpha$ -PD-1 groups were 20, 22, 26, and 34 days, respectively. Compared with  $^{125}\text{I}$  RPI and  $\alpha$ -PD-1, combination therapy resulted in significantly longer survival ( $P = 0.0026$  and  $P = 0.0019$ , respectively; Fig. 2D). These results suggest that anti-PD-1 therapy can improve the efficacy of  $^{125}\text{I}$  RPI and combination therapy can induce the abscopal effect and improve the prognosis in mice.

## Combination Therapy Increases Proliferation And Activation Of Cd8 + tils

To determine whether combination therapy could activate anti-tumor immunity, we analyzed T lymphocytes in the TME. Mice treated with  $^{125}\text{I}$  RPI or anti-PD-1 had a slightly increased proportion of CD8 + TILs ( $P = 0.4103$  and  $P = 0.6318$ , respectively), but those treated with combination therapy had significantly increased numbers of CD8 + TILs ( $P < 0.05$  compared with all other groups; Fig. 3A and 3B). There was no difference in the proportion of CD4 + TILs among the groups ( $P = 0.1539$ ,  $^{125}\text{I}$  RPI +  $\alpha$ -PD-1 vs. PBS; Fig. 3A and 3B). To evaluate the activity of CD8 + TILs, we analyzed the ability of CD8 + TILs to produce IFN- $\gamma$  and TNF- $\alpha$  (Fig. 3C). There were approximately five-fold more IFN- $\gamma$  + CD8 + TILs in the  $^{125}\text{I}$  RPI +  $\alpha$ -PD-1 group than in the PBS group (Fig. 3D;  $P = 0.0013$ ), and six-fold more TNF- $\alpha$  + CD8 + TILs than in the PBS group (Fig. 3D;  $P = 0.0002$ ). These results showed that combined therapy could activate anti-tumor immunity and increase the number and activity of T cells in the TME. We also showed that the immune activation effect of  $^{125}\text{I}$  RPI is achieved through PD-1 blockade.

### Combined therapy reduces the number of Tregs in the TME

Tregs can promote tumor growth by inhibiting T cell activation(25). Studies have found that RT can upregulate the expression of Tregs in the TME(13), but anti-PD-1 treatment can reduce the expression of Tregs(26). However, the effect of  $^{125}\text{I}$  RPI and  $^{125}\text{I}$  RPI combined with anti-PD-1 treatment on Tregs is unknown. To this end, we analyzed the proportion of Tregs and showed that  $^{125}\text{I}$  RPI did not affect the proportion of Tregs ( $P = 0.2442$ ). The proportion of Tregs decreased after anti-PD-1 treatment ( $P = 0.0051$ ), but the decrease was more significant after the combined treatment (Fig. 4A and 4B;  $P = 0.0227$ ). We further analyzed the ratio of CD8 + T/Tregs, which was significantly higher in the  $^{125}\text{I}$  RPI +  $\alpha$ -PD-1 group than in the other groups ( $P < 0.05$  compared with all other groups; Fig. 4B). These results suggest that combination therapy could reshape T cell immunity and make the tumor immune microenvironment into one of immune activation.

### The schedule is a critical determinant affecting the efficacy of combination therapy

The sequence of RT and anti-PD-1 treatment affects the efficacy of the combined therapy. Previous studies showed that concurrent therapy is better than sequential therapy(12, 27–29). To determine

whether administration of  $^{125}\text{I}$  RPI or  $\alpha$ -PD-1 mAb at different times affects the efficacy of combination therapy, we examined three different combination schedules:  $^{125}\text{I}$  RPI followed after three days by  $\alpha$ -PD-1 mAb (schedule A); concurrent administration of  $\alpha$ -PD-1 mAb and  $^{125}\text{I}$  RPI (schedule B); and  $\alpha$ -PD-1 mAb followed after three days by  $^{125}\text{I}$  RPI (schedule C) (Fig. 5A). The treatment start time of the three schedules was on day 10 after injection of the tumor cells. The median survival time for schedules B and C were 34 and 33 days, respectively, while schedule A reduced the survival time compared to  $^{125}\text{I}$  RPI only ( $P = 0.0128$ , 22 days vs. 26 days; Fig. 5B). In schedule A,  $\alpha$ -PD-1 mAb did not control tumor growth, demonstrating that when  $^{125}\text{I}$  RPI was used at a later stage, the tumor burden was already too high. This could explain why schedule A was less efficient. These results suggest that initiating  $^{125}\text{I}$  RPI earlier to delay tumor progression represents a more effective combination schedule.

## Discussion

In this study, we used a lung cancer model to demonstrate PD-1/PD-L1 inhibition of the anti-tumor immune response caused by  $^{125}\text{I}$  RPI. On day 6 after  $^{125}\text{I}$  RPI, PD-L1 expression was upregulated, but PD-1 expression was not. On day 12, PD-L1 was further upregulated; PD-1 expression was also upregulated. After  $^{125}\text{I}$  RPI combined with anti-PD-1 therapy, the immunosuppressive state was reversed, the infiltration of CD8 + T cells in the TME increased nearly two-fold, and the proportion of Tregs reduced three-fold, which significantly inhibited growth of the primary and second tumors. In addition, we showed that the sequence of  $^{125}\text{I}$  RPI and anti-PD-1 therapy affects the efficacy of the combined therapy, and delaying  $^{125}\text{I}$  RPI reduces the efficacy of combination therapy.

PD-1 is a surface marker of exhausted T cells. Our results showed that the proportion of CD8 + PD-1 + TILs did not increase on day six after  $^{125}\text{I}$  RPI, but increased significantly on day 12. The expression of PD-L1 on tumor cells also increased on day 12 after  $^{125}\text{I}$  RPI. This indicates that with increasing time after particle implantation and radiation dose accumulation, T cell function is gradually impaired, limiting the immune activation effect of  $^{125}\text{I}$  RPI. Our results show that  $^{125}\text{I}$  RPI combined with anti-PD-1 therapy can significantly inhibit the growth of the primary tumor and can also induce the abscopal effect, which can inhibit the growth of secondary tumors, whereas  $^{125}\text{I}$  RPI treatment alone cannot produce the abscopal effect. We showed that combination therapy can reduce immune suppression and activate systemic anti-tumor immune responses.

The results achieved were further verified by the flow cytometry results. The proportion of CD8 + TILs in the TME increased significantly following the combined therapy, and the ability of CD8 + TILs to secrete IFN- $\gamma$  and TNF- $\alpha$  was also significantly enhanced. This indicated an increase in infiltrated T cells in the TME and, therefore, enhanced activity and killing ability. Schau et al. showed that a single dose of 15 Gy increased the expression of Tregs in mouse melanoma, but two fractions of 7.5 Gy reduced the expression of Treg(30). In our study, the proportion of Tregs did not increase or decrease after  $^{125}\text{I}$  brachytherapy characterized by hyperfractionation, but decreased in combination with anti-PD-1 therapy. It is worth noting that the ratio of CD4 + TILs did not increase after the combined treatment. One

explanation is that Tregs accounted for ~ 21% of CD4 + T cells in the PBS group, compared with ~ 7% in the  $^{125}\text{I}$  RPI +  $\alpha$ -PD-1 group. The decrease in Tregs resulted in no change in the total number of CD4 + T cells, which masked the increase of effector CD4 + T cells. Another explanation is that CD4 + T cells are not the effector cells of  $^{125}\text{I}$  RPI when combined with anti-PD-1 therapy, so there was no increase. Many preclinical studies have found that CD4 + T cells are dispensable for RT combined with anti-PD-1 therapy, and depletion of CD4 + T cells did not affect the efficacy of the combined treatment, whereas CD8 + T cells are essential(12, 14).

Dovedi et al. found that administration of  $\alpha$ -PD-L1 mAb seven days after completion of RT did not produce an effective anti-tumor immune response(12). His results showed that the synergistic effect of RT and immunotherapy has a time limit, and concurrent therapy is better than sequential therapy. In our study, the  $\alpha$ -PD-1 mAb administered three days after  $^{125}\text{I}$  RPI did not affect the efficacy of the combination therapy, possibly because the  $^{125}\text{I}$  RPI and anti-PD-1 therapy have a longer synergistic time window. However, administration of  $^{125}\text{I}$  RPI after dosing with three days of  $\alpha$ -PD-1 mAb did reduce the efficacy. Our results are consistent with the study of Ahmed et al. where patients with non-small cell lung cancer (NSCLC) who received RT before or during the administration of anti-PD-1 had significantly longer survival than patients who received RT after anti-PD-1 therapy(28). This may be because radiation can promote the release of antigens, and this is conducive to the early initiation of anti-tumor immunity(31). In addition,  $\alpha$ -PD-1 mAb is only moderately effective and cannot significantly inhibit tumor growth. When  $^{125}\text{I}$  particles are implanted, the tumor burden is too high, and  $^{125}\text{I}$  RPI is a low-dose-rate RT. Dosage accumulation takes time, and this causes the tumor volume to be significantly inhibited within the experimental endpoint.

Clinical studies have found that single anti-PD-1/PD-L1 treatment does not have a curative effect in all cancer patients, and the objective response rate of NSCLC is < 20%(32). Studies have shown that anti-PD-1/PD-L1 therapy is beneficial in supporting sufficient numbers of T cells in the TME(33). The immune promotion effect of RT can turn a drug-resistant population of anti-PD-1/PD-L1 into one that is beneficial(34). Clinical studies have proven that RT is an independent predictor of good prognosis for anti-PD-1/PD-L1 therapy in the treatment of NSCLC(35). Synergistic differences for anti-PD-1 treatment between different segmentation modes remain unknown. Here, we provide data on hyperfractionated brachytherapy combined with anti-PD-1/PD-L1 therapy. In terms of synergistic effects with immunotherapy,  $^{125}\text{I}$  RPI has unique advantages over EBRT. First, it is highly conformable; during EBRT normal tissues also receive radiation, resulting in a decrease in radiosensitive lymphatic immune cells in these normal tissues, whereas normal tissues do not receive any radiation during brachytherapy. Also, the radiation radius of  $^{125}\text{I}$  is only 1.7 cm, and the radiation intensity decreases as the distance increases, protecting normal tissues from radiation damage(36). Second, it has an ultra-long half-life;  $^{125}\text{I}$  can provide ~ 180 days of irradiation, which can continuously promote tumor immunity. Anti-PD-1/PD-L1 treatment mostly uses disease progression or unacceptable toxicity as the withdrawal criteria. The time window for the synergistic effect between  $^{125}\text{I}$  RPI and anti-PD-1/PD-L1 therapy is longer, resulting in longer anti-tumor immunity.

This study has some limitations. Although some immunophenotypes have been detected, additional intrinsic mechanisms need to be further explored. The effective radiation time of  $^{125}\text{I}$  RPI is 180 days. An increase in the cumulative dose may enhance the curative effect. However, due to the limited survival time of tumor-bearing mice, it was not possible to monitor the synergistic effect of  $^{125}\text{I}$  RPI and anti-PD-1 therapy over a longer time. We did not conduct any toxicity experiments, but no obvious toxicity was observed during our experiments. Also, our study has not been verified in other tumor models. We believe that  $^{125}\text{I}$  RPI combined with anti-PD1 has broad applications in solid tumors, and especially in prostate cancer. Prostate cancer is less sensitive to anti-PD-1/PD-L1 treatment(37, 38), but clinical trials have shown that activated T cells increase in the peripheral blood of prostate cancer patients gradually and continuously after  $^{125}\text{I}$  RPI(39).  $^{125}\text{I}$  RPI may improve the effect of prostate cancer immunotherapy.

## Conclusion

This study shows that  $^{125}\text{I}$  RPI combined with anti-PD-1/PD-L1 can significantly inhibit tumor growth and enhance anti-tumor immunity in mice. In addition, the efficacy is affected by the timing of  $^{125}\text{I}$  RPI treatment. Although the potential advantages of  $^{125}\text{I}$  RPI combined with anti-PD-1/PD-L1 treatment still need to be confirmed when compared with EBRT combined with anti-PD-1/PD-L1, our results for hyperfractionated brachytherapy combined with anti-PD-1/PD-L1 treatment are promising and lay the foundation for future clinical applications.

## Abbreviations

RT: Radiotherapy;  $^{125}\text{I}$  RPI: Iodine-125 particle implantation; LLC: Lewis lung cancer; TME: tumor microenvironment; Tregs: T regulatory cells; EBRT: external beam RT; NSCLC: non-small cell lung cancer.

## Declarations

Ethics approval and consent to participate

All animal experiments were approved by the Guidelines of the First Affiliated Hospital of Chongqing Medical University Biomedical Ethics Committee.

Consent for publication

Not applicable

Availability of data and materials

All data generated or analyzed during this study are included in this published article.

Competing interests

The authors declare that they have no competing interests.

## Funding

The authors received no financial support for the research, authorship, and/or publication of this article.

## Authors' contributions

Yiyi Cao, ZhengJie Wang and Hua Pang were involved in the conception and the study design.

Yiyi Cao, Wenbo Li, Jia Li and Yu Weng performed the experiments and data acquisition.

Yiyi Cao drafted the manuscript under ZhengJie Wang and Hua Pang mentorship. Yiyi Cao and Chang Chen performed statistical analyses. All authors reviewed the manuscript, read, and approved the final manuscript.

## Acknowledgments

The authors gratefully acknowledge the assistance of the Department of Nuclear Medicine, First Affiliated Hospital of Chongqing Medical University, Institute of Radiation Oncology Laboratory and Animal Experiment Center of Chongqing Medical University.

## References

1. Chen LP, Flies DB. Molecular mechanisms of T cell co-stimulation and co-inhibition. *Nat Rev Immunol.* 2013;13(4):227-42.
2. Wu X, Zhang H, Xing Q, Cui J, Li J, Li Y, et al. PD-1(+) CD8(+) T cells are exhausted in tumours and functional in draining lymph nodes of colorectal cancer patients. *British journal of cancer.* 2014;111(7):1391-9.
3. Gong J, Chehrazi-Raffle A, Reddi S, Salgia R. Development of PD-1 and PD-L1 inhibitors as a form of cancer immunotherapy: a comprehensive review of registration trials and future considerations. *Journal for immunotherapy of cancer.* 2018;6:18.
4. Demaria S, Ng B, Devitt ML, Babb JS, Kawashima N, Liebes L, et al. Ionizing radiation inhibition of distant untreated tumors (abscopal effect) is immune mediated. *Int J Radiat Oncol Biol Phys.* 2004;58(3):862-70.
5. Hodge JW, Sharp HJ, Gameiro SR. Abscopal regression of antigen disparate tumors by antigen cascade after systemic tumor vaccination in combination with local tumor radiation. *Cancer biotherapy & radiopharmaceuticals.* 2012;27(1):12-22.
6. Schumacher TN, Schreiber RD. Neoantigens in cancer immunotherapy. *Science.* 2015;348(6230):69-74.
7. Sethuraman SN, Ranjan A. Neoantigen activation, protein translocation and targeted drug delivery in combination with radiotherapy. *Therapeutic delivery.* 2016;7(6):377-85.

8. Formenti SC, Demaria S. Combining radiotherapy and cancer immunotherapy: a paradigm shift. *J Natl Cancer Inst.* 2013;105(4):256-65.
9. Messmer D, Yang H, Telusma G, Knoll F, Li J, Messmer B, et al. High mobility group box protein 1: an endogenous signal for dendritic cell maturation and Th1 polarization. *Journal of immunology (Baltimore, Md : 1950).* 2004;173(1):307-13.
10. Aymeric L, Apetoh L, Ghiringhelli F, Tesniere A, Martins I, Kroemer G, et al. Tumor cell death and ATP release prime dendritic cells and efficient anticancer immunity. *Cancer Res.* 2010;70(3):855-8.
11. Obeid M, Tesniere A, Ghiringhelli F, Fimia GM, Apetoh L, Perfettini JL, et al. Calreticulin exposure dictates the immunogenicity of cancer cell death. *Nature medicine.* 2007;13(1):54-61.
12. Dovedi SJ, Adlard AL, Lipowska-Bhalla G, McKenna C, Jones S, Cheadle EJ, et al. Acquired resistance to fractionated radiotherapy can be overcome by concurrent PD-L1 blockade. *Cancer Res.* 2014;74(19):5458-68.
13. Muroyama Y, Nirschl TR, Kochel CM, Lopez-Bujanda Z, Theodoros D, Mao W, et al. Stereotactic Radiotherapy Increases Functionally Suppressive Regulatory T Cells in the Tumor Microenvironment. *Cancer immunology research.* 2017;5(11):992-1004.
14. Deng L, Liang H, Burnette B, Beckett M, Darga T, Weichselbaum RR, et al. Irradiation and anti-PD-L1 treatment synergistically promote antitumor immunity in mice. *J Clin Invest.* 2014;124(2):687-95.
15. Park SS, Dong H, Liu X, Harrington SM, Krco CJ, Grams MP, et al. PD-1 Restrains Radiotherapy-Induced Abscopal Effect. *Cancer immunology research.* 2015;3(6):610-9.
16. Dewan MZ, Galloway AE, Kawashima N, Dewynngaert JK, Babb JS, Formenti SC, et al. Fractionated but not single-dose radiotherapy induces an immune-mediated abscopal effect when combined with anti-CTLA-4 antibody. *Clin Cancer Res.* 2009;15(17):5379-88.
17. Vanpouille-Box C, Alard A, Aryankalayil MJ, Sarfraz Y, Diamond JM, Schneider RJ, et al. DNA exonuclease Trex1 regulates radiotherapy-induced tumour immunogenicity. *Nat Commun.* 2017;8:15.
18. Yamamoto Y, Offord CP, Kimura G, Kuribayashi S, Takeda H, Tsuchiya S, et al. Tumour and immune cell dynamics explain the PSA bounce after prostate cancer brachytherapy. *British journal of cancer.* 2016;115(2):195-202.
19. Dai F, Wang J, An H, Lei T, Tang K, Ma X, et al. Therapy of (125)I particles implantation inhibited the local growth of advanced non-small cell lung cancer: a retrospective clinical study. *American journal of translational research.* 2019;11(6):3737-49.
20. Liu Q, Dai X, Zhou X, Ye F, Zhou Y. Comparison of TACE combined with and without iodine-125 seeds implantation therapy for advanced stage hepatocellular carcinoma: a systematic review and meta-analysis. *Journal of BUON : official journal of the Balkan Union of Oncology.* 2019;24(2):642-9.
21. Huang W, Lu J, Chen KM, Wu ZY, Wang QB, Liu JJ, et al. Preliminary application of 3D-printed coplanar template for iodine-125 seed implantation therapy in patients with advanced pancreatic cancer. *World journal of gastroenterology.* 2018;24(46):5280-7.
22. Shaverdian N, Lisberg AE, Bornazyan K, Veruttipong D, Goldman JW, Formenti SC, et al. Previous radiotherapy and the clinical activity and toxicity of pembrolizumab in the treatment of non-small-

- cell lung cancer: a secondary analysis of the KEYNOTE-001 phase 1 trial. *The Lancet Oncology*. 2017;18(7):895-903.
23. Anderson ES, Postow MA, Wolchok JD, Young RJ, Ballangrud A, Chan TA, et al. Melanoma brain metastases treated with stereotactic radiosurgery and concurrent pembrolizumab display marked regression; efficacy and safety of combined treatment. *Journal for immunotherapy of cancer*. 2017;5(1):76.
  24. Takamori S, Toyokawa G, Takada K, Shoji F, Okamoto T, Maehara Y. Combination Therapy of Radiotherapy and Anti-PD-1/PD-L1 Treatment in Non-Small-cell Lung Cancer: A Mini-review. *Clinical lung cancer*. 2018;19(1):12-6.
  25. Tanaka A, Sakaguchi S. Regulatory T cells in cancer immunotherapy. *Cell research*. 2017;27(1):109-18.
  26. Sasidharan Nair V, Elkord E. Immune checkpoint inhibitors in cancer therapy: a focus on T-regulatory cells. *Immunology and cell biology*. 2018;96(1):21-33.
  27. Kotecha R, Kim JM, Miller JA, Juloori A, Chao ST, Murphy ES, et al. The impact of sequencing PD-1/PD-L1 inhibitors and stereotactic radiosurgery for patients with brain metastasis. *Neuro-Oncology*. 2019;21(8):1060-8.
  28. Ahmed KA, Kim S, Arrington J, Naghavi AO, Dilling TJ, Creelan BC, et al. Outcomes targeting the PD-1/PD-L1 axis in conjunction with stereotactic radiation for patients with non-small cell lung cancer brain metastases. *J Neuro-Oncol*. 2017;133(2):331-8.
  29. Murphy B, Walker J, Bassale S, Monaco D, Jaboin J, Ciporen J, et al. Concurrent Radiosurgery and Immune Checkpoint Inhibition Improving Regional Intracranial Control for Patients With Metastatic Melanoma. *Am J Clin Oncol-Cancer Clin Trials*. 2019;42(3):253-7.
  30. Schae D, Ratikan JA, Iwamoto KS, McBride WH. Maximizing tumor immunity with fractionated radiation. *International journal of radiation oncology, biology, physics*. 2012;83(4):1306-10.
  31. Tang C, Wang X, Soh H, Seyedin S, Cortez MA, Krishnan S, et al. Combining radiation and immunotherapy: a new systemic therapy for solid tumors? *Cancer immunology research*. 2014;2(9):831-8.
  32. Garon EB, Rizvi NA, Hui R, Leighl N, Balmanoukian AS, Eder JP, et al. Pembrolizumab for the treatment of non-small-cell lung cancer. *N Engl J Med*. 2015;372(21):2018-28.
  33. Chen DS, Mellman I. Elements of cancer immunity and the cancer-immune set point. *Nature*. 2017;541(7637):321-30.
  34. Teng MW, Ngiow SF, Ribas A, Smyth MJ. Classifying Cancers Based on T-cell Infiltration and PD-L1. *Cancer Res*. 2015;75(11):2139-45.
  35. Yamaguchi O, Kaira K, Hashimoto K, Mouri A, Miura Y, Shiono A, et al. Radiotherapy is an independent prognostic marker of favorable prognosis in non-small cell lung cancer patients after treatment with the immune checkpoint inhibitor, nivolumab. *Thoracic cancer*. 2019.
  36. Patel RB, Baniel CC, Sriramaneni RN, Bradley K, Markovina S, Morris ZS. Combining brachytherapy and immunotherapy to achieve in situ tumor vaccination: A review of cooperative mechanisms and

clinical opportunities. Brachytherapy. 2018;17(6):995-1003.

37. Hansen AR, Massard C, Ott PA, Haas NB, Lopez JS, Ejadi S, et al. Pembrolizumab for advanced prostate adenocarcinoma: findings of the KEYNOTE-028 study. *Annals of oncology : official journal of the European Society for Medical Oncology*. 2018;29(8):1807-13.
38. Fay AP, Antonarakis ES. Blocking the PD-1/PD-L1 axis in advanced prostate cancer: are we moving in the right direction? *Annals of translational medicine*. 2019;7(Suppl 1):S7.
39. Kubo M, Satoh T, Ishiyama H, Tabata KI, Tsumura H, Komori S, et al. Enhanced activated T cell subsets in prostate cancer patients receiving iodine-125 low-dose-rate prostate brachytherapy. *Oncology reports*. 2018;39(1):417-24.
40. The English in this document has been checked by at least two professional editors, both native speakers of English. For a certificate, please see: <http://www.textcheck.com/certificate/uKaFuq>

## Figures

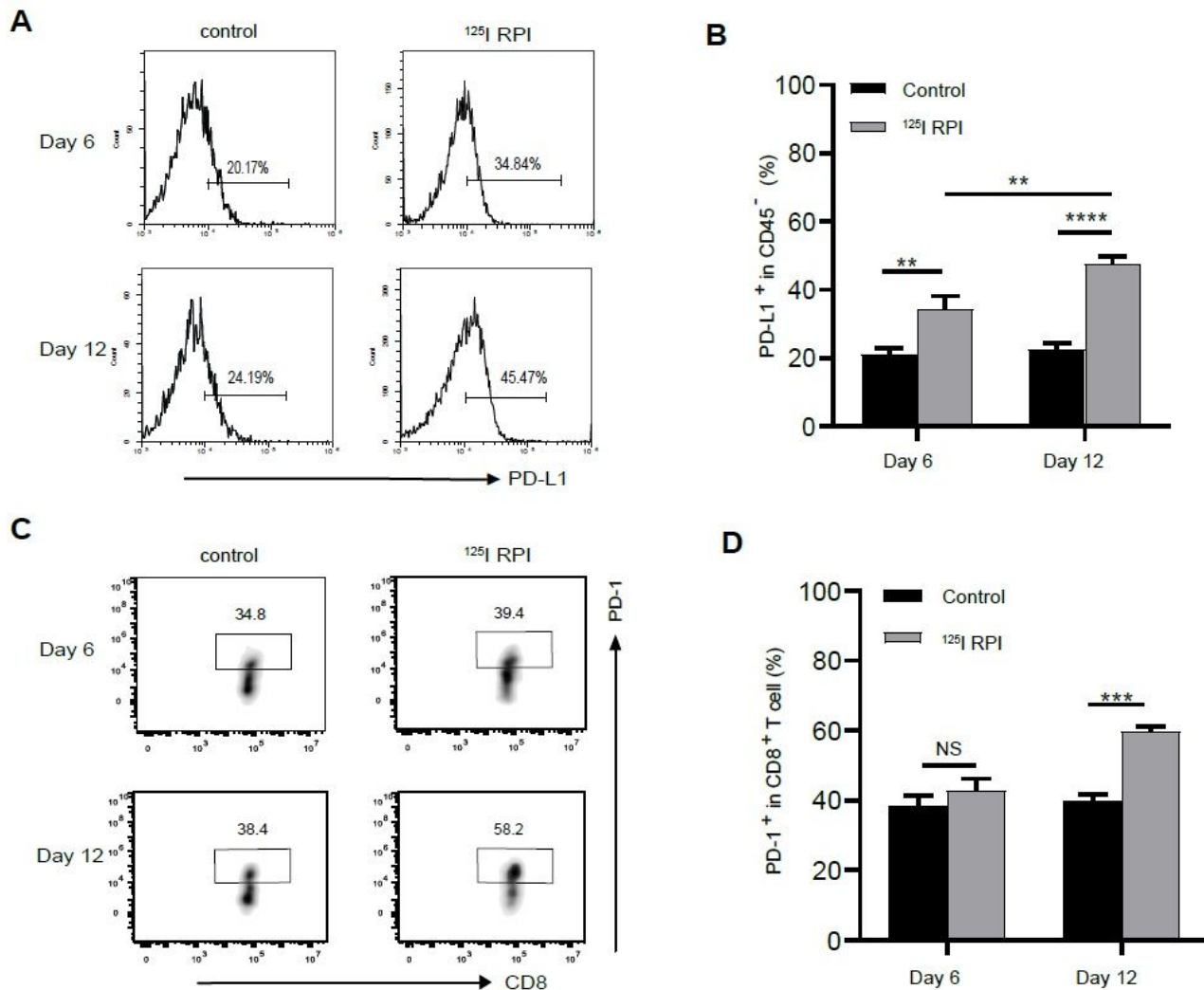
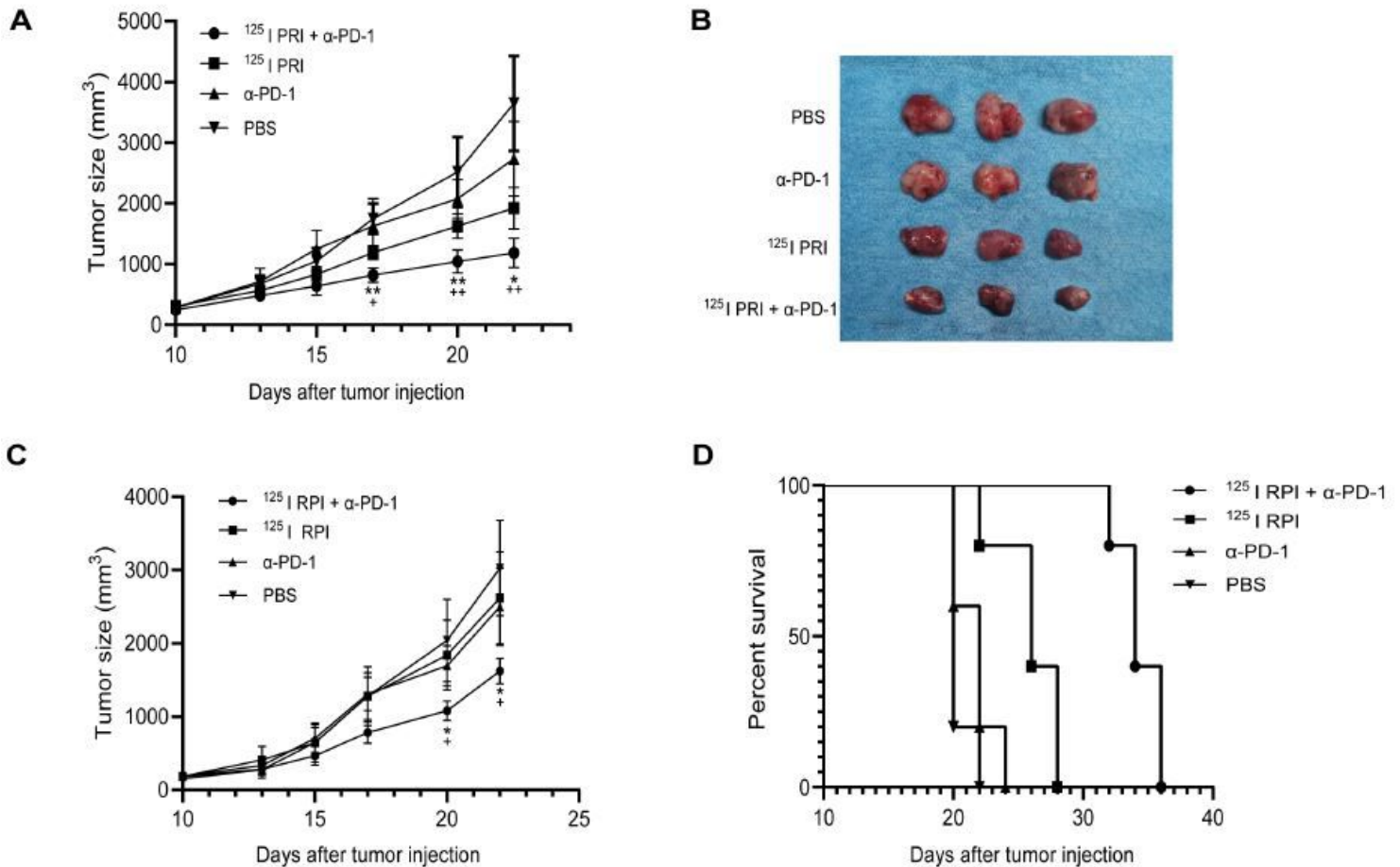


Figure 1

125I RPI upregulated the expression of PD-1/PD-L1. C57BL/6 mice were injected with LLC cells ( $1 \times 10^6$ ) SC into the right hindlimb. On days 6 and 12 after 125I RPI, tumors were removed to obtain cell suspensions for surface staining. Flow cytometry to detect PD-1 and PD-L1 expression is shown. (A) PD-L1 expression on tumor cells (CD45-). (B) Quantitative data of the percentage of PD-L1+ cells relative to tumor cells. (C) PD-1 expression on CD8+ T cells. (D) Quantitative data of the percentage of PD-1+ cells relative to CD8+ T cells. Numbers of mice per group were 3–4; \* $P < 0.05$ ; \*\* $P < 0.01$ ; \*\*\* $P < 0.001$ ; and NS, not significant.



**Figure 2**

125I RPI and anti-PD-1 therapy synergistically enhanced the anti-tumor effect. A total of  $1 \times 10^6$  LLC cells were injected SC into the right hindlimb (primary tumor) of C57BL/6 mice on day 0, and into the left flanks (secondary tumor) on day 3. On day 10, the primary tumor was treated with 125I RPI and/or 200  $\mu$ g  $\alpha$ -PD-1 mAb or PBS.  $\alpha$ -PD-1 mAb or PBS was injected IP every other day for five instances. (A) Tumor growth curve of the primary tumor. (B) Primary tumors were harvested on day 22. Only three representative tumors from each group are shown. (C) Tumor growth curve of the secondary tumor. (D) The Kaplan–Meier method was used to monitor the survival of tumor-bearing mice. Numbers of mice per group were 5–7. +/\* $P < 0.05$ ; ++/\*\* $P < 0.01$ ; \* significance when compared with 125I RPI mice; + significance when compared with  $\alpha$ -PD-1 mice.

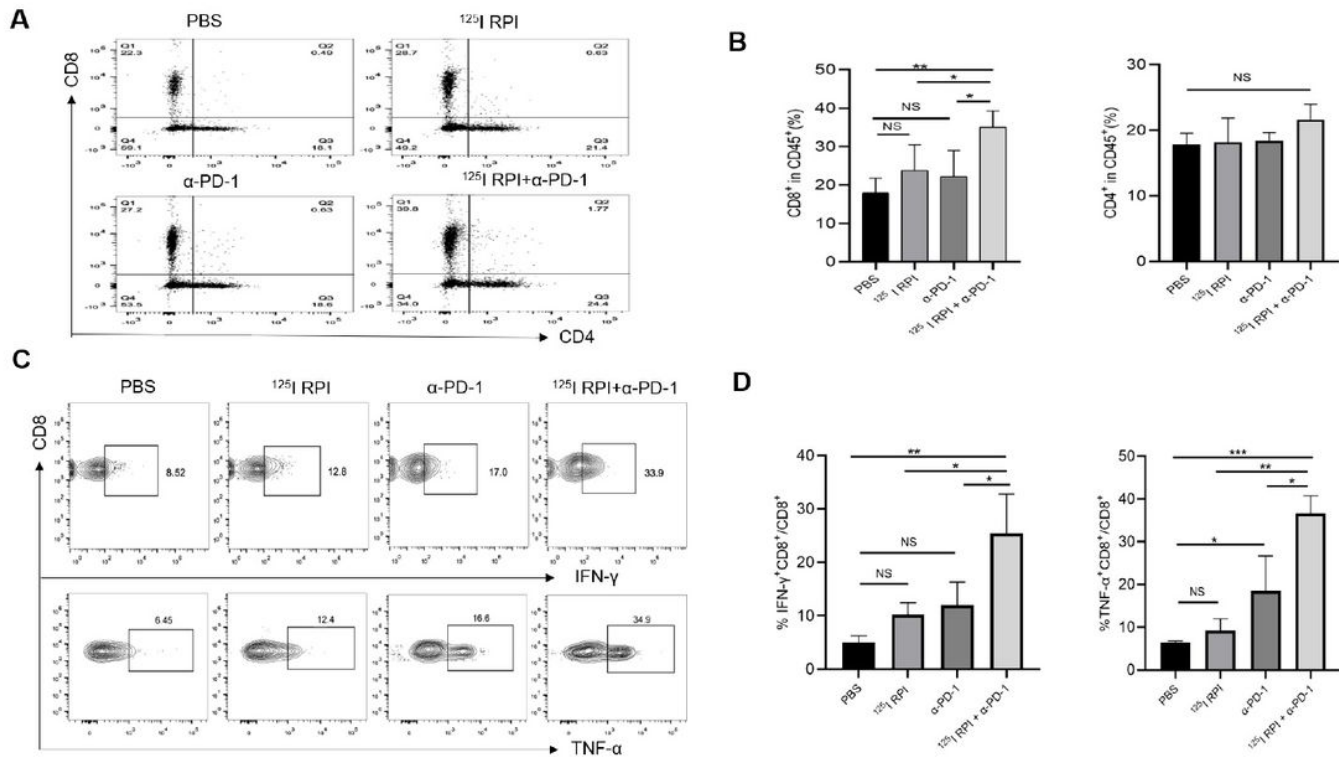


**Figure 3**

125I RPI combined with anti-PD-1 therapy promotes proliferation and activation of CD8<sup>+</sup> TILs. Tumors were removed 12 days after treatment to obtain cell suspensions for staining. Flow cytometric analysis of CD4<sup>+</sup> T and CD8<sup>+</sup> T gated on CD45<sup>+</sup> cells in tumors. (B) Quantitative data of the percentage of CD8<sup>+</sup> T cells and CD4<sup>+</sup> T cells relative to CD45<sup>+</sup> cells. (C) Flow cytometric analysis of IFN-γ and TNF-α gated on CD8<sup>+</sup> cells in tumors. (D) Quantitative data of the percentage of IFN-γ<sup>+</sup> CD8<sup>+</sup> T cells and TNF-α<sup>+</sup> CD8<sup>+</sup> T cells relative to CD8<sup>+</sup> T cells. Numbers of mice per group were 3–4; \*P < 0.05; \*\*P < 0.01; \*\*\*P < 0.001; and NS, not significant.

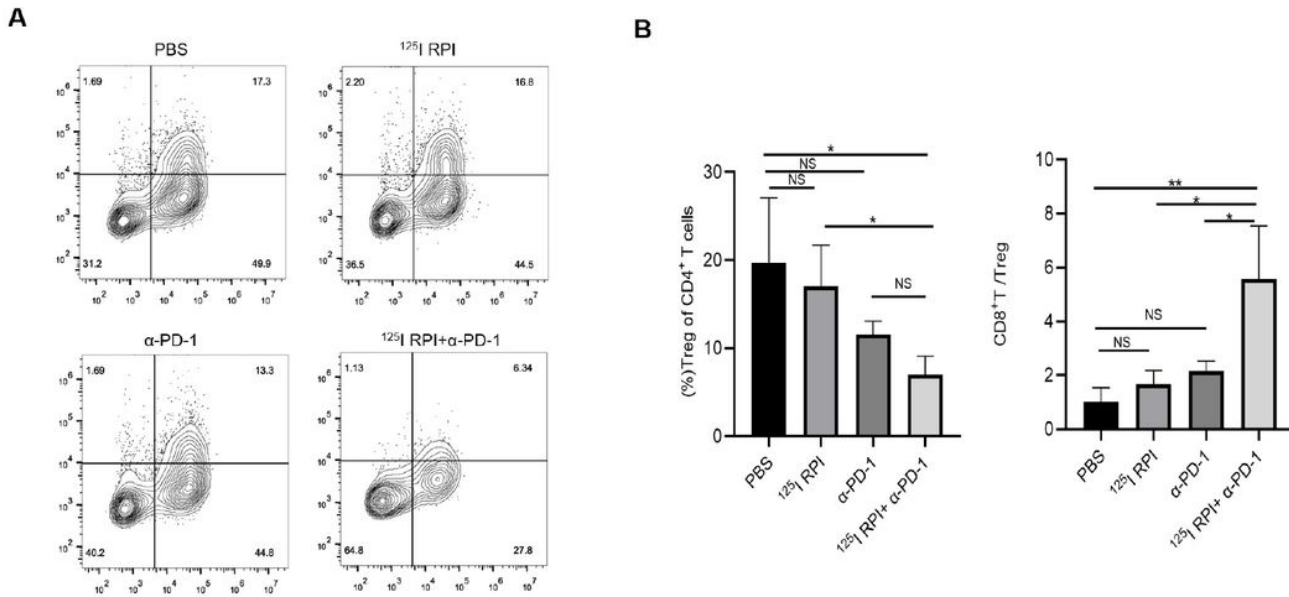


**Figure 4**

$^{125}\text{I}$  RPI combined with anti-PD-1 reduced the proportion of Tregs in the TME. (A) Flow cytometric analysis of Tregs (CD4+ CD25+ Foxp3+). (B) Quantitative data of the percentage of Treg cells relative to CD4+ T cells and the ratio of CD8+ T cells to Treg cells. Numbers of mice per group were 3–4; \* $P < 0.05$ ; \*\* $P \leq 0.01$ ; and NS, not significant.

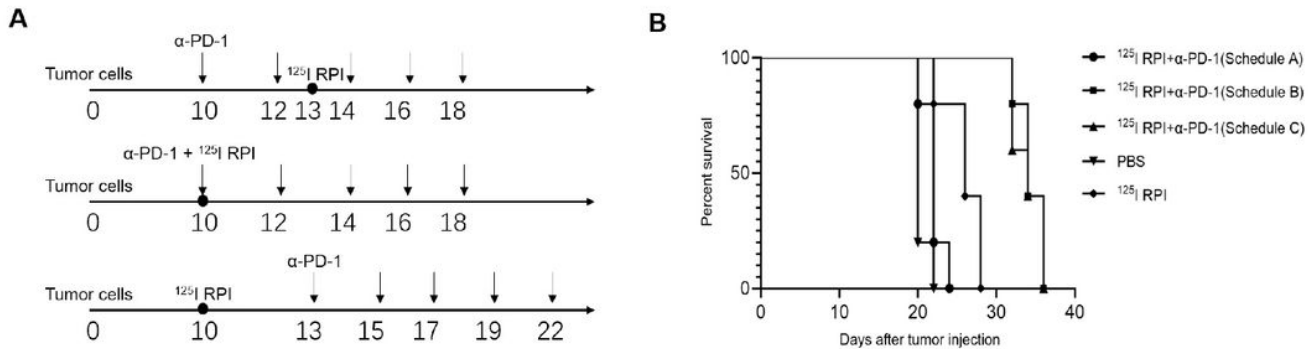


**Figure 5**

The sequence of  $^{125}\text{I}$  RPI and anti-PD-1 therapy affects the efficacy of the combined therapy. (A) Schematic diagram of the three combination schedules. (B) The survival of tumor-bearing mice was analyzed by Kaplan–Meier analysis.